Front. Med. 2021, 15(1): 43–52
https://doi.org/10.1007/s11684-020-0769-6

REVIEW

Applications of atomic force microscopy in immunology

Jiping Li[1], Yuying Liu[2,3], Yidong Yuan[1,4], Bo Huang (✉)[2,3,5]

[1]Beijing Smartchip Microelectronics Technology Company Limited, Beijing 100192, China; [2]Department of Immunology & National Key Laboratory of Medical Molecular Biology, Institute of Basic Medical Sciences, Chinese Academy of Medical Sciences, School of Basic Medicine Peking Union Medical College, Beijing 100005, China; [3]Clinical Immunology Center, Chinese Academy of Medical Sciences, Beijing 100005, China; [4]School of Microelectronics, Tianjin University, Tianjin 300072, China; [5]Department of Biochemistry & Molecular Biology, Tongji Medical College, Huazhong University of Science & Technology, Wuhan 430030, China

Abstract **Cellular mechanics, a major regulating factor of cellular architecture and biological functions, responds to intrinsic stresses and extrinsic forces exerted by other cells and the extracellular matrix in the microenvironment. Cellular mechanics also acts as a fundamental mediator in complicated immune responses, such as cell migration, immune cell activation, and pathogen clearance. The principle of atomic force microscopy (AFM) and its three running modes are introduced for the mechanical characterization of living cells. The peak force tapping mode provides the most delicate and desirable virtues to collect high-resolution images of morphology and force curves. For a concrete description of AFM capabilities, three AFM applications are discussed. These applications include the dynamic progress of a neutrophil-extracellular-trap release by neutrophils, the immunological functions of macrophages, and the membrane pore formation mediated by perforin, streptolysin O, gasdermin D, or membrane attack complex.**

Keywords cellular mechanics; atomic force microscopy; neutrophil extracellular trap; macrophage phagocytosis; pore formation

Introduction

Immunology research focuses on biochemical stimuli to study the biological behaviors of cells but often overlooks the physical or mechanical cues from the biological microenvironments. However, the mechanical behavior of cells is a major regulating factor of cellular architectures and biological functions [1–3]. The cells exert mechanical forces to mediate complex immune responses and respond to mechanical stimulation as part of their normal physiologic functions. Atomic force microscopy (AFM) has emerged as a major surface scanning tool to measure cellular mechanics with unprecedented advantages, such as easy sample preparation, noninvasive imaging in ambient environments, and high-resolution imaging for topology and force measurements [4–7]. This review elaborates the principles of cellular mechanics and AFM measurements and examines their tactics in observing the formation of neutrophil extracellular traps (NETs) or NETosis, macrophage phagocytosis, and the process of membrane pore formation to facilitate the understanding of advanced AFM techniques in immunology research.

Received September 25, 2019; accepted March 4, 2020
Correspondence: Bo Huang, tjhuangbo@hotmail.com

Principle of cellular mechanics

Cells respond to mechanical stimuli through cytoskeletal reorganization and force generation in a mechanical microenvironment [8,9]. The cytoskeleton, a major physical element of cells, is not a fixed structure but a dynamic and adaptive skeleton that spatially organizes component polymers and regulatory proteins, thereby physically and biochemically responding to environmental cues and generating alternate cellular configurations and movements. The three main cytoskeletal polymers within a cell are microtubules, actin filaments, and intermediate filaments, and like nuclear skeleton, they may exhibit different mechanical properties (such as stiffness). These polymers establish an essential network architecture with complex assembly and disassembly dynamics, creating various ways to transmit compressive and tensile stresses

throughout the whole cell and controlling the cell's morphology and mechanics, such as cell elasticity, viscosity, or viscoelasticity [10]. A disruption of the cytoskeletal architecture by genetic disorders or pathogens can alter cellular mechanical properties [11–15]. The distress in the mechanical microenvironment can also profoundly influence cellular behavior [16–19]. Therefore, an understanding of the principle of cellular mechanics undoubtedly provides new insights into the strategies for disease diagnosis and treatment.

The human body has evolved a set of essential protective mechanisms against infections, injury, and cancer, in which a series of innate immune cells, such as neutrophils, macrophages, dendritic cells, and adaptive immune cells (including T and B cells) are utilized [20–23]. At the lesion site, immune cells initially recognize pathogen-associated molecular patterns (PAMPs) or damage-associated molecular patterns through pattern-recognition receptors (PRRs), e.g., toll-like receptors (TLRs) [24,25]. After binding to TLRs, the environmental inflammatory signals are transduced to trigger an immune response, thereby clearing nonself substances, such as pathogenic organisms. Besides this PRR-based chemical reaction, cells apply contractile forces to sense the mechanical signal of the surrounding microenvironment and respond accordingly. The binding of the extracellular matrix (ECM) proteins, such as collagen and fibrin, to integrins leads to mechanotransduction along the clustered integrins to the focal adhesions (FAs) [26]. Thus, the outside mechanical signals are sensed at FAs and can be converted into biochemical signals inside the cells. Cooperating with the chemical signal, this mechanical signal may allow immune cells to rapidly migrate, phagocytose, and clear foreign materials. For example, during T cell activation, when the immune synapse intensifies after 30 min of cell contact, the interacting force between the T cells receptor (TCR) and MHC-antigenic peptide complex reaches about 14 nN peak value, which is required for immune synapse formation and subsequent T cell activation [27]. Following the T cell activation, perforin is released into the intercellular space of the immune synapse, causing pores to form. These pores allow the entry of granzymes into the target cell. However, drilling a hole in the membrane of target cells, which is widely viewed as a chemical process, involves physical and mechanical forces [28,29]. Therefore, the cellular mechanics, which represents cellular responses to intrinsic stresses and extrinsic forces, plays a critical role in concerted immune response.

Measurement of cellular mechanics by AFM

Different cell types have different degrees of stiffness, which is widely used to define cellular mechanics. Moreover, the stiffness of a cell should match the ECM stiffness to properly sense and respond to the surrounding mechanical signal [30,31]. Cellular stiffness is determined by tensile stress. Myosin II uses its ATPase activity to hydrolyze ATP and release energy, thus resulting in the generation of tensile stress by actin microfilament structures in a cell. The activation of the myosin-based contraction increases the tensile force in actin filaments, which stiffens the F-actin lattice. Thus, the cell stiffness is the collective result of actin polymerization and myosin II-mediated contractile activation.

Several methods have been developed to measure cellular stiffness [31,32]. One is the magnetic twisting cytometry (MTC) technique, which has been used to study the mechanical behavior of cells on the basis of twisting ligand-coated magnetic microbeads bound to membrane receptors and measuring the bead rotation with a magnetometer or with the displacement of the bead center of mass. Cells ubiquitously express integrins. Thus, the ferromagnetic beads coated with the RGD (Arg–Gly–Asp) tripeptide can be used to attach to cell surfaces, which are subjected to a magnetic field to deform the cell membrane locally. The distortion range can be measured and calculated to describe the cell stiffness or mechanical force [33]. AFM is another widely used method to measure cell stiffness. Unlike MTC, AFM scans the cell surface and directly measures the cell stiffness. AFM is invented by Binnig *et al.* following the appearance of a series of scanning probe microscopes, such as the scanning tunneling microscope and scanning near-field optical microscope, introduced in the 1980s [4]. AFM characterizes with minimal sample preparation and analysis in a normal ambient environment (i.e., without freezing, metal coating, vacuum pumping, or cell staining), and the probe scan can obtain surface topography at the nanometer (or even angstrom) scale resolution and quantitative mechanical forces at piconewton force sensitivity simultaneously. This method promises noninvasive imaging and force measurements of cellular mechanics.

Compared with AFM, optical microscopes have a relatively low image resolution (to hundred nanometers), are limited by the wavelength of the light source, and cannot be used to visualize small samples, like viruses with sizes ranging from 20 nm to 400 nm [5,20]. Also, cell staining is usually required in optical microscopes for better observation. Electron microscopy may obtain high-resolution images at the nanoscale level, but these approaches require a vacuum chamber and dedicated procedures for sample preparation and analysis, such as tissue sectioning and a plunge frozen process in transmission electron microscopy [34]. Some limitations also exist for AFM. First, AFM, a surface scanning approach only, cannot monitor activities inside the cells. However, optical and fluorescence microscopy may be used to observe additional details of intracellular activities [14,35–37]. Second, the sample cells in some experimental

environments, such as liquid, are usually mobile, and cell drifts can inhibit the investigation of long-term adhesion. The destructive chemical or physical immobilization of cells may be required for studying cellular mechanics [4,12,38]. Third, the measurement throughput of AFM is low (about one cell for every 10 minutes). Thus, researchers are exploring spiral scanning instead of the conventional zigzag raster pattern to speed up measurements [39–41]. Overall, the advanced force–distance curve-based AFM is a powerful technique to measure mechanical forces, including Young's modulus, viscoelasticity, adhesion, and cell deformities.

AFM principle and its running modes

The basic AFM configuration contains four major parts (Fig. 1): a probe as one complete cantilever with a sharp tip mounted at its end, a piezoelectric actuator that drives the probe, a laser source, and a position-sensitive detector (PSD). Any cantilever bending is detected by the PSD deflection signal of a weak laser beam, which is reflected off the back of the cantilever and originates from the laser source. As the probe tip scans a sample in close proximity, the quantitative mechanical interactions between the probe tip and the sample surface are measured by PSD signals, and the sample 3D topography can be plotted by recording the z-piezo movements of the tip in accordance with the *x*–*y* horizontal coordinates in raster scanning. The force–distance curve (Fig. 2) can be extracted when the probe tip taps the sample surface. When approaching the sample surface, the probe tip experiences an attractive force until the contact point is reached, which is followed by a growing repulsive force representing the indentation depth into the sample. When retracting the probe back, the probe tip experiences a descending repulsive force first, and a growing adhesive forces up to its maximum adhesion before being restored to the tip's initial equilibrium position. Based on this principle, several AFM models have been developed to quantitate the mechanical properties of sample surfaces, including deformation, Young's modulus, adhesion force, and energy dissipation (Fig. 2) [4,32,42].

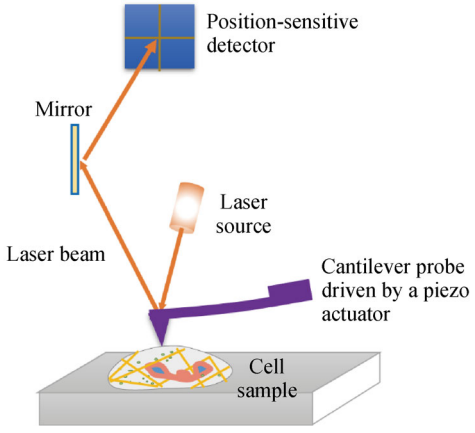

Fig. 1 Basic atomic force microscope (AFM) setup: a cantilever probe, a piezoelectric actuator (not drawn), a laser source, and a position-sensitive detector.

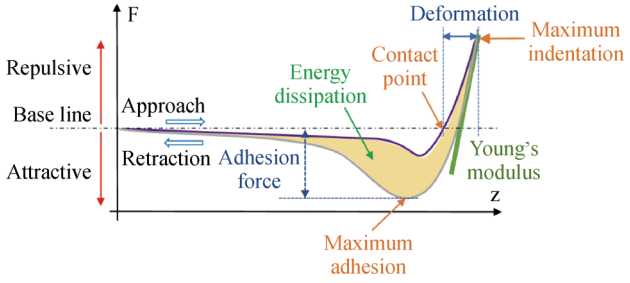

Fig. 2 Force–distance curve by AFM. In one measurement cycle, the probe approaches the sample to make a tip–sample contact and then retracts for a complete graph of tip force interactions, where Young's modulus (by the linear slope), membrane deformation (by the maximum indentation), adhesion force (by the maximum adhesion point), and energy dissipation (by the enclosed area) can be extracted.

In the contact mode AFM, a tiny vertical force is directly and continuously applied using the probe tip on the contact surface, and a repulsive interaction can be measured using the displacement of the cantilever free-end. As the probe gently traces over the sample surface, the flexible cantilever accommodates topology changes with the vertical force, and the vulnerable biological sample suffers from the possible damages created by the vertical force and the accompanying frictional force [5,6].

In the tapping mode AFM, the probe tip comes into contact with the sample surface intermittently. In this mode, the cantilever is oscillated at a predefined amplitude (normally tens of nanometers) and frequency (at or near its resonance frequency) normal to the sample surface, thereby avoiding the problems of lateral forces and dragging across the sample surface. The tapping mode AFM ensures good topology measurements and creates negligible friction and shear forces, which are desirable for biological research [43,44]. The tapping mode AFM operates at a cantilever resonant frequency and does not directly measure the interaction forces for feedback control, which is somewhat vulnerable to complicated cantilever dynamics on soft samples and may miss information about single interactions.

The peak force tapping mode AFM presents further improvements, including a fixed oscillation frequency, which is far less than the probe cantilever resonant frequency. Also, a fixed peak force of the force–distance curve after tip–sample contact enhances imaging feedback, and the vertical piezoelectric actuator (z-piezo) is driven in

a sinusoidal manner [32,42]. This kind of operation skillfully suppresses the long-range interactions (i.e., adhesive and electrostatic forces) between the tip and the sample surface for height control, reduces artificial errors linked to the complex tip–surface interactions and cantilever dynamics, and improves the image quality of ultrasoft samples (about 1 kPa) to rigid samples (up to 100 GPa). The topography, adhesion, and stiffness maps of a sample surface can be captured simultaneously, and only tiny forces at levels lower than other modes are exerted on the delicate biological samples.

Currently, advanced AFM approaches offer researchers unprecedented opportunities to image biological samples and probe their mechanical properties with high resolution in their functional and physiologic environments. The measurements are nondestructive and can be implemented in ambient environments or in aqueous solutions at room temperature. Furthermore, the AFM probe tips can be mounted with single cells or functionalized with chemicals or biomolecules to detect cell–cell or specific molecular interactions, which greatly extend AFM applications for biological research [45–49]. The time-efficient and controlled temporal recording of a series of force curves can be used to visualize the biological processes of cells.

However, some basic points should be kept in mind to get successful and accurate measurements. First, defective laboratory environments may impair the measurement. The precise AFM instrument is sensitive to any environmental vibration, and experiments are recommended to be implemented in an acoustic isolation box. Humidity control is needed because moisture may condense on the tip with capillary force, which may overwhelm other force contributions [38]. Temperature fluctuations should also be avoided because the cantilever has different top and bottom faces (top faces are usually coated with gold for good light reflection) and may bend in accordance with temperature changes [4]. Second, the tip shape and the cantilever mechanics should be chosen properly and calibrated correctly before use. The sample's mechanical properties especially the Young's modulus strongly depend on the tip shape, and tip wear is one major reason for measurement failures. The spring constant of the AFM cantilever should be comparable with the stiffness of biological cell samples, which ranges from 0.01 N/m to 0.5 N/m. Third, the condition of the cell culture medium during AFM measurement evidently influences cellular mechanics. Temperature variations may alter the cytoskeleton structures, leading to changes in cellular mechanics [32]. Intriguingly, reducing the serum concentration in a cell's culture medium has decreased the cellular Young's modulus in Nikkhah *et al.*'s experiments [50]. Fourth, standard cell fixation with formaldehyde or glutaraldehyde is often used to simplify the experiment and improve imaging resolution, but many studies show that this strategy may alter cellular mechanics by increasing cell stiffness and impairing cell viability [12].

Application of AFM to observe NETosis

AFM is an invaluable tool for obtaining high-resolution topographical images and has a wide range of applications in immunology. Apart from phagocytosis and the generation of reactive oxygen species, NETs are recognized as a major defense pathway for neutrophilic granulocytes to capture and eliminate pathogens. During NETosis, neutrophils experience apparent and successive cellular and subcellular morphology changes, histone modifications, chromatin decondensation, and release of 3D fibrous mesh traps composed of chromatin and antimicrobial components. Neubert *et al.* have used AFM for the characterization of the NETosis process to measure the changes in morphology and cellular mechanics and organized the process into three distinct phases with no return (Fig. 3), namely, P1 (before chromatin swelling), P2 (chromatin expansion), and P3 (membrane rupture and NET release)

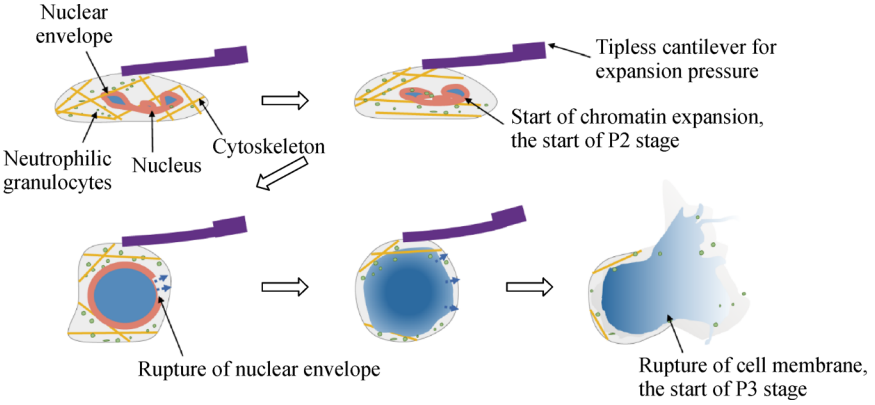

Fig. 3 NETosis process and entropic swelling of chromatin. The process can be divided into three distinct phases with no return in accordance with the chromatin status.

[51]. Using AFM, the PMA-stimulated cells are observed to adhere and flatten (about 4 μm height) in P1 and then round up ($>$ 8 μm height) in P2 prior to the membrane rupture in P3, whereas the control cells have remained nearly round and are about 7 μm to 8 μm high. Although AFM is incapable of observing the chromatic swelling inside the cells, the live-cell confocal laser scanning microscopy and various fluorescence labeling methods have been used to visualize and quantify the nuclear envelope rupture and chromatic expansion inside the cell membranes.

For the force measurements by AFM, the expansion pressure during the P2 stage can be directly characterized. The physical swelling of chromatin with biochemically modified histones governs this process. A tipless cantilever with a large contact area is used to manually approach a single cell until cell contact is observed, and the cantilever is passively deflected by the cell rounding process until the final rupture of cell membrane (at pressure of 80–170 Pa), during which the entropic swelling pressure can be extracted from the cantilever deflection measurements. Also, the cell elasticity measurements and the decrease in the Young's modulus from 1.5 kPa in P1 to 0.3 kPa in P2 have corroborated the dissolution of the major cell cytoskeletal components, such as F-actin and the microtubule apparatus. This dissolution facilitates soft cellular mechanics and membrane rupture during the NETosis process especially in the P2 stage. The membrane tension or plasma membrane tension in cells is the sum of the inner membrane tension and the adhesion energy per unit area from the membrane-to-cortex attachments [52,53]. The membrane tension measurements by AFM [51], which has shown a decrease from 0.35 mN/m to 0.07 mN/m, affirm the disassembly of the actin cortex beneath the cell membrane and the membrane reorganization during NETosis. These experiments exhibit the capability and limitations of AFM-based morphology and mechanical force measurements for the study of neutrophils during the NETosis process. AFM is a powerful assistant for the understanding of these biological progresses.

Application of AFM to observe the physiologic functions of macrophages

The macrophages differentiated from blood monocytes in circulation are professional phagocytic cells, which recognize, ingest, and digest cellular debris and pathogens [54–56]. These macrophages are distributed throughout the tissues in the body, where they make adherent contact with diverse ECMs. As such, the macrophages' cytoskeletons are modified and can dynamically respond to environmental cues. Thus, the tension in the plasma membrane influences the whole cellular deformation process through membrane–cytoskeleton adhesion. As verified by AFM measurements [57], the murine macrophages show a 49% increase in the Young's modulus after 48 h in culture, when adhered to an ECM-coated substrate rather than an uncoated control substrate. And a 47% decrease in the Young's modulus is observed when the ones adhered to the ECM-coated substrate are treated with cytochalasin D for 15 min. These results provide clear evidence of cytoskeleton reorganization in macrophages. Similar to FAs, podosomes (or invadopodia) are integrin-containing adhesion structures that contact ECMs. Podosomes are also involved in ECM degradation via a belt-shape rosette and characterized by a core of column-shaped F-actin perpendicularly anchored into the substratum via integrins, vinculin, talin, and paxillin. This dynamic podosome protrusive force is considered to be an efficient way for macrophages to probe microenvironments and progress into its appropriate forms during cellular migration, differentiation, and morphogenesis. The heights of podosome protrusions can be determined using an innovative and specified setup named protrusion force microscopy (PFM). In PFM, macrophages are placed onto the compliant Formvar sheet, and the measured protrusion force increases with the substratum stiffness and exhibits the combined oscillatory activities of actomyosin contraction and actin polymerization within a constant period [56]. In addition, the micropatterned fibrinogen has been applied to confine podosome formation and facilitate the AFM analyses of podosome height and stiffness with nanoscale accuracy, and their temporal dynamics in living macrophages are demonstrated [58].

Macrophages exhibit apparent morphological membrane changes to ingest and digest cellular debris or pathogen particles. Thus, macrophage morphology is considered an efficient sensor for extracellular and intracellular stimuli. In this regard, fluorescence AFM, an integrated platform equipped with an advanced AFM and an inverted optical microscope, is developed to image the steps macrophages undergo during the phagocytosis of fungal pathogens with nanoscale structural details of cellular morphology [20]. The main steps of phagocytosis under observation include macrophage infection, internalization of yeast cells, intracellular hyphal growth and germ tube formation, and pathogen escape. AFM helps to capture the nanoscale features of the macrophage surface structures, such as ruffles, lamellipodia, filopodia, phagocytic cups, and membrane remnants, whereas fluorescence imaging helps discern cells under pathogen–host interactions at a microscale level. AFM has revealed that the macrophage surface is always rough and is adorned with many dorsal "ruffles" with height of 100–500 nm, reflecting the presence of podosomes, which is difficult to detect by optical microscopy. The subsequent escape of the *Candida albicans* hyphae, which is characterized by a smooth and featureless morphology, demonstrates that the surface discrimination of phagocytic cells can be easily

captured by AFM. This approach allows the discernment of internalized and externalized hyphal cells and the visualization of macrophage debris following membrane rupture and the malicious fungal strategy to mask its PAMPs to avoid recognition by the immune system. Hence, the nanoimaging platform of correlated fluorescence AFM demonstrates great capabilities to facilitate nanomedicine research into understanding and controlling fungal infections.

Application of AFM to visualize immune-mediated membrane pore formation

Membrane pore formation is recognized as a major cell death-mediating mechanism of immune cells in pathogen clearance and the pathogenesis of inflammatory diseases. Upon interacting with target cells (tumor or virus-infected cells), the effector $CD8^+$ T cells release perforin and granzymes into the intercellular immune synapse, where perforin acts as an executioner to drill a hole in the membrane of target cells (Fig. 4A) [59–61]. Besides perforin, the complement-induced membrane attack complex (MAC) and gasdermins (GSDMs) are the principal executioners responsible for the membrane pore formation of the target pathogen-laden or transformed cells [28,62–64]. However, past investigations into the mechanisms of pore formation are based on defective scanning microscopy, such as cryo-electron microscopy, to image the pores formed on two-dimensional artificial liposomes, not true live cellular membranes, where vacuum pumping, tissue sectioning, or plunge frozen process may be involved. For the observation of pores on live cells, high-resolution (nanometer scale) microscopy and the gentle handling of cells under ambient conditions are stringently required. General scanning electron microscopy is not applicable here. Furthermore, the use of liposomes instead of actual cell membranes for pore visualization ignores important cellular components, like membrane proteins and the underlying cytoskeleton, leading to conceivable errors in observing the dynamic process of pore formation.

Our recent studies have explored the extraordinary capabilities of AFM to perform high-resolution and noninvasive imaging of the dynamic pore formation process mediated by executioner molecules [29]. The findings reveal the real-time morphology and mechanical responses of true cell membranes during pore formation, substantially improving our understanding of pore formation-mediated cell death in immune surveillance, such as during the clearance of pathogens or tumor cells (Fig. 4). The peak force tapping mode AFM is used to capture the height profiles and the adhesion and the stiffness maps of cell membrane pores precisely and simultaneously (Fig. 4B). These results are sufficient for pore topography recognition. The pores formed in the target cell membranes are usually characterized by steep trenches in the surface morphology. The peak force tapping mode AFM is nicely adapted to accommodate this situation with very low probe forces and high-resolution imaging because this mode is insensitive to these geometric effects and has no difficulty probing the bottom of trenches. The NanoScope Analysis 1.8 is used to analyze the images collected by AFM. Utilizing the section analysis supplied by this software, which is typically used for the analysis of surface

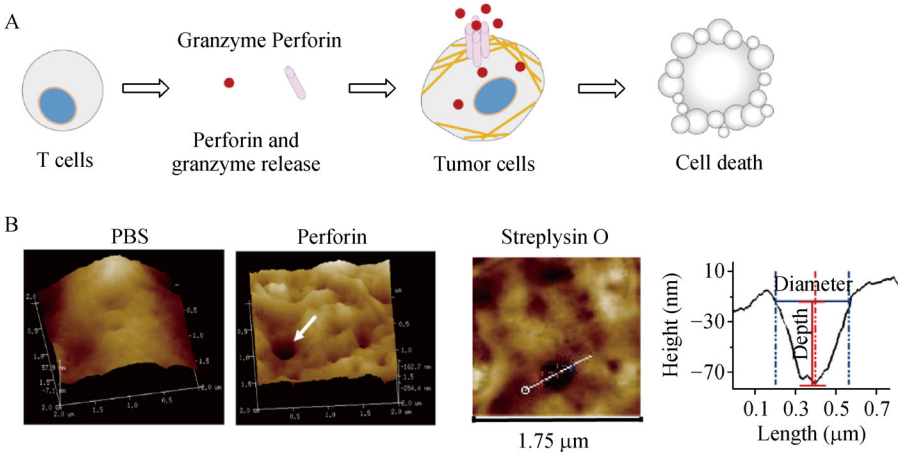

Fig. 4 SLO/perforin-mediated membrane pore formation. (A) Principle of perforin-induced pore formation and cell death. (B) Surface roughness and topography measurements of OVA-B16 cells treated with PBS, perforin (50 U), and streplysin O (SLO) (50 U) isolated from activated human $CD8^+$ T cells for 5 min. The white line across the pore image on the SLO-treated cell indicates the location for topography measurements on the right. The pore depth is defined as the vertical distance between the two red horizontal lines on the curve diagram, and the pore diameter is defined as the horizontal distance between the two dotted blue vertical lines. This result is from Liu *et al*. (*Cell Mol Immunol*. 2019;16:611. Open Access.)

roughness, the recorded curve reflects the moving track of the tip. The images show U-type curves with a flat bottom, indicating that a pore structure is detected by the tip, which can precisely illustrate the size and the depth of the formed pores. In our experiments, the AFM is equipped with a 90 μm piezoelectric scanner (0.4 N/m for nominal spring constant) and a sharpened silicon tip (2 nm for nominal radius) in an acoustic isolation box, and the cantilever oscillation frequency, oscillation amplitude, and the maximum probe force during AFM measurements are set to 2 kHz, 50 nm, and 1 nN, respectively. The ambient temperature is maintained at 20–24 °C. Also, membrane-impermeable dyes, such as PI, are applied to assist in discerning pores from pits.

The activated $CD8^+$ cytotoxic T cells release perforin and granzymes into the immune synapse, where perforin drills holes in the membrane of target cells. Like perforin, the bacterium-derived toxin streptolysin O (SLO) is capable of forming pores in the target membrane of bacterial cells. Perforin and SLO are applied to the OVA-B16 melanoma tumor cells for the visualization of pore formation, and the pore-like structures are observed clearly. Here, live and dead cells that are fixed using 4% paraformaldehyde are imaged using AFM and have exhibited large pores in their cell membranes. The AFM tip (NPG-10) is functionalized with the anti-SLO antibody, and this probe is applied to image the SLO-treated cells in accordance with the protocol published by Newton *et al*. to confirm that these pores are induced by the toxic protein SLO [65]. Then, the SLO antibody-conjugated NPG-10 tips are used to image the SLO-treated OVA-16 cells by using AFM. The force–distance curve-based AFM height and adhesion maps are uploaded into the NanoScope software. Results show that the force curves generated from the areas without pores do not experience a rupture, but the curves from the border with pores have clear ruptures, suggesting that single or multiple antigen-antibody bonds are formed. As such, SLO is localized around the pores.

A previous study has shown that the pore size induced by perforin is around 200 nm in real cells, which is bigger than the size detected from the artificial lipid monolayer (around 20 nm) [28,66]. Such a difference may be ascribed to the membrane structure. The artificial lipid monolayer is lacking protein molecules, whereas the real cell membrane contains many membrane proteins. Perforin interacts with the membrane lipid molecules to form pores. Thus, when exerting an effect on an artificial liposome, perforin simply interacts with lipid molecules, and no protein-mediated cytoskeletal change generating force is observed. However, perforin interacts with lipid in an authentic cell membrane and real protein molecules, leading to the activation of the cytoskeleton and causing force generation. An opposing force may act on the perforin molecule, leading to its conformation change and the subsequent formation of a large pore. In addition, the pore variation, which is detected in our study, may be ascribed to the dynamic action of perforin. With a short perforin treatment, small-sized pores are formed, whereas a long treatment time has resulted in large pores [29]. Sometimes, adjacent pores may fuse to form a large pore due to the membrane dynamics, further exacerbating the pore variation. As such, these processes may contribute to the large pore formation.

The pore formation process is time-dependent, and the target membranes become rougher and more porous with longer perforin or SLO treatment time. Additionally, an impressive cell repair process following pore formation is observed in a dose- and time-dependent manner. A threshold dosage of SLO is required for pore formation in the target cell membranes. Following the removal of SLO from the culture medium, pores decrease gradually in size, depth, and number. Additionally, the surface roughness of the target cells' membranes has decreased, and the pores finally disappear after 2 h of cell repair. Large pores (over hundreds of nanometers) are minimally repaired, resulting in cell death. Therefore, clear and dynamic pore-forming and pore-repairing processes can be observed using the AFM topology measurements.

Immune studies have highlighted the critical role of the GSDM family members in the membrane pore formation process [34,63]. When activated by inflammatory caspases (caspase-1, caspase-4, caspase-5, and caspase-11) or caspase-3, GSDM D or E mediates pyroptotic cell death through oligomer insertion and pore formation in the cellular membranes. The necroptotic cell death involves the activation of the receptor-interacting protein kinases (RIP) 1/RIP3/mixed lineage kinase domain-like (MLKL) pathway and the MLKL-mediated pore formation in the plasma membrane [67,68]. Besides pyroptosis or necroptosis, which mediates monocyte/macrophage inflammatory death to fight against certain pathogenic infections, the MAC derived from complement components (i.e., C5b, C6, C7, C8, and C9) in innate immunity results in pore formation in the membrane but kills pathogenic cells. In our experiments, an apparent swollen morphology (> 80 μm in size) and the subsequent bursting of the target cells following active GSDM E transduction are observed. The dynamic complement-mediated pore formation process in real cells is also visualized for the first time. Results exhibit the powerful capability of AFM-based morphological observations and mechanical force measurements, suggesting that AFM is a powerful tool for the study of the immune system.

Conclusions

Studies on cellular mechanics extend new perspectives on the essential cellular, subcellular, and intercellular

functions involved in immune responses, which are related to the processes of immune cell proliferation, adhesion, migration, apoptosis, antigen recognition, and pathogen clearance. The mechanical properties of cells and tissues exhibit remarkable variable physical performances under healthy homeostasis and are known to reflect the pathological states of many human diseases, including cancer metastasis, inflammation, viral infection, and frailty in aging. AFM, an important experimental tool, exhibits great potential for the mechanical characterization of cells during immune responses. Advanced AFM techniques, such as peak force tapping approaches, provide nanometer resolution and piconewton forces for cell morphology and stiffness measurements, which adapt to the scale of cells and the magnitude of their intercellular forces. In addition, AFM enables noninvasive and nondestructive measurements with minimal sample preparations under ambient conditions or in aqueous culture media at room temperature, significantly magnifying its advantages for an authentic live study of biological functions. The visualization of dynamic NETosis, macrophage phagocytosis, membrane pore formation processes, and other immunology phenotypes (e.g., the activation of essential eosinophils [69], the osteogenesis of bone implant materials [70], and the effects of anti-inflammatory drugs) [71] certify the powerful capability of AFM for morphological and mechanical force measurements. The current and future applications of AFM in immunology research are encouraging and will undoubtedly bring new insights into the principles of the immune system.

Acknowledgements

This work was supported by the National Natural Science Foundation of China (No. 81788101) and the Chinese Academy of Medical Sciences Initiative for Innovative Medicine (CAMS-I2M) (No. 2016-I2M-1-007). This work was partially supported by the project of "Research on the Passive Micro Sensor Components and Systems Applied in SF6 Detection" (No. 54681618002400k0000000).

Compliance with ethics guidelines

Jiping Li, Yuying Liu, Yidong Yuan, and Bo Huang declared no conflict of interest. This manuscript is a review article and does not involve a research protocol requiring approval by the relevant institutional review board or ethics committee.

References

1. Miller CJ, Davidson LA. The interplay between cell signalling and mechanics in developmental processes. Nat Rev Genet 2013; 14 (10): 733–744
2. Mohammadi H, Sahai E. Mechanisms and impact of altered tumour mechanics. Nat Cell Biol 2018; 20(7): 766–774
3. Roca-Cusachs P, Conte V, Trepat X. Quantifying forces in cell biology. Nat Cell Biol 2017; 19(7): 742–751
4. Butt HJ, Cappella B, Kappl M. Force measurements with the atomic force microscope: technique, interpretation and applications. Surf Sci Rep 2005; 59(1–6): 1–152
5. Chang KC, Chiang YW, Yang CH, Liou JW. Atomic force microscopy in biology and biomedicine. Tzu Chi Medical J 2012; 24(4): 162–169
6. Maver U, Velnar T, Gaberšček M, Planinšek O, Finšgar M. Recent progressive use of atomic force microscopy in biomedical applications. Trends Analyt Chem 2016; 80: 96–111
7. Wu Y, Cai J, Cheng L, Xu Y, Lin Z, Wang C, Chen Y. Atomic force microscope tracking observation of Chinese hamster ovary cell mitosis. Micron 2006; 37(2): 139–145
8. Fletcher DA, Mullins RD. Cell mechanics and the cytoskeleton. Nature 2010; 463(7280): 485–492
9. Atilla-Gokcumen GE, Muro E, Relat-Goberna J, Sasse S, Bedigian A, Coughlin ML, Garcia-Manyes S, Eggert US. Dividing cells regulate their lipid composition and localization. Cell 2014; 156(3): 428–439
10. Moeendarbary E, Harris AR. Cell mechanics: principles, practices, and prospects. Wiley Interdiscip Rev Syst Biol Med 2014; 6(5): 371–388
11. Kasas S, Dietler G. Probing nanomechanical properties from biomolecules to living cells. Pflugers Arch 2008; 456(1): 13–27
12. Braet F, Taatjes DJ, Wisse E. Probing the unseen structure and function of liver cells through atomic force microscopy. Semin Cell Dev Biol 2018; 73: 13–30
13. Calvo F, Ege N, Grande-Garcia A, Hooper S, Jenkins RP, Chaudhry SI, Harrington K, Williamson P, Moeendarbary E, Charras G, Sahai E. Mechanotransduction and YAP-dependent matrix remodelling is required for the generation and maintenance of cancer-associated fibroblasts. Nat Cell Biol 2013; 15(6): 637–646
14. Wang N, Zhang M, Chang Y, Niu N, Guan Y, Ye M, Li C, Tang J. Directly observing alterations of morphology and mechanical properties of living cancer cells with atomic force microscopy. Talanta 2019; 191: 461–468
15. Alcaraz J, Otero J, Jorba I, Navajas D. Bidirectional mechanobiology between cells and their local extracellular matrix probed by atomic force microscopy. Semin Cell Dev Biol 2018; 73: 71–81
16. Harris MJ, Wirtz D, Wu PH. Dissecting cellular mechanics: Implications for aging, cancer, and immunity. Semin Cell Dev Biol 2019; 93: 16–25
17. Elosegui-Artola A, Andreu I, Beedle AEM, Lezamiz A, Uroz M, Kosmalska AJ, Oria R, Kechagia JZ, Rico-Lastres P, Le Roux AL, Shanahan CM, Trepat X, Navajas D, Garcia-Manyes S, Roca-Cusachs P. Force triggers YAP nuclear entry by regulating transport across nuclear pores. Cell 2017; 171(6): 1397–1410.e14
18. Madl CM, Heilshorn SC, Blau HM. Bioengineering strategies to accelerate stem cell therapeutics. Nature 2018; 557(7705): 335–342
19. Krieg M, Dunn AR, Goodman MB. Mechanical control of the sense of touch by β-spectrin. Nat Cell Biol 2014; 16(3): 224–233
20. El-Kirat-Chatel S, Dufrêne YF. Nanoscale imaging of the *Candida*-macrophage interaction using correlated fluorescence-atomic force microscopy. ACS Nano 2012; 6(12): 10792–10799
21. Pageon SV, Govendir MA, Kempe D, Biro M. Mechanoimmunology: molecular-scale forces govern immune cell functions. Mol Biol

Cell 2018; 29(16): 1919–1926
22. Nakamura K, Smyth MJ. Myeloid immunosuppression and immune checkpoints in the tumor microenvironment. Cell Mol Immunol 2020; 17(1): 1–12
23. Kim YB, Ahn YH, Jung JH, Lee YJ, Lee JH, Kang JL. Programming of macrophages by UV-irradiated apoptotic cancer cells inhibits cancer progression and lung metastasis. Cell Mol Immunol 2019; 16(11): 851–867
24. Liu CH, Liu H, Ge B. Innate immunity in tuberculosis: host defense vs pathogen evasion. Cell Mol Immunol 2017; 14(12): 963–975
25. Li Y, Li Y, Cao X, Jin X, Jin T. Pattern recognition receptors in zebrafish provide functional and evolutionary insight into innate immune signaling pathways. Cell Mol Immunol 2017; 14(1): 80–89
26. Kechagia JZ, Ivaska J, Roca-Cusachs P. Integrins as biomechanical sensors of the microenvironment. Nat Rev Mol Cell Biol 2019; 20 (8): 457–473
27. Hosseini BH, Louban I, Djandji D, Wabnitz GH, Deeg J, Bulbuc N, Samstag Y, Gunzer M, Spatz JP, Hämmerling GJ. Immune synapse formation determines interaction forces between T cells and antigen-presenting cells measured by atomic force microscopy. Proc Natl Acad Sci USA 2009; 106(42): 17852–17857
28. Leung C, Hodel AW, Brennan AJ, Lukoyanova N, Tran S, House CM, Kondos SC, Whisstock JC, Dunstone MA, Trapani JA, Voskoboinik I, Saibil HR, Hoogenboom BW. Real-time visualization of perforin nanopore assembly. Nat Nanotechnol 2017; 12(5): 467–473
29. Liu Y, Zhang T, Zhou Y, Li J, Liang X, Zhou N, Lv J, Xie J, Cheng F, Fang Y, Gao Y, Wang N, Huang B. Visualization of perforin/gasdermin/complement-formed pores in real cell membranes using atomic force microscopy. Cell Mol Immunol 2019; 16(6): 611–620
30. Discher DE, Mooney DJ, Zandstra PW. Growth factors, matrices, and forces combine and control stem cells. Science 2009; 324 (5935): 1673–1677
31. Wu PH, Aroush DRB, Asnacios A, Chen WC, Dokukin ME, Doss BL, Durand-Smet P, Ekpenyong A, Guck J, Guz NV, Janmey PA, Lee JSH, Moore NM, Ott A, Poh YC, Ros R, Sander M, Sokolov I, Staunton JR, Wang N, Whyte G, Wirtz D. A comparison of methods to assess cell mechanical properties. Nat Methods 2018; 15(7): 491–498
32. Li M, Dang D, Liu L, Xi N, Wang Y. Atomic force microscopy in characterizing cell mechanics for biomedical applications: a review. IEEE Trans Nanobioscience 2017; 16(6): 523–540
33. Zhang Y, Wei F, Poh YC, Jia Q, Chen J, Chen J, Luo J, Yao W, Zhou W, Huang W, Yang F, Zhang Y, Wang N. Interfacing 3D magnetic twisting cytometry with confocal fluorescence microscopy to image force responses in living cells. Nat Protoc 2017; 12(7): 1437–1450
34. Sborgi L, Rühl S, Mulvihill E, Pipercevic J, Heilig R, Stahlberg H, Farady CJ, Müller DJ, Broz P, Hiller S. GSDMD membrane pore formation constitutes the mechanism of pyroptotic cell death. EMBO J 2016; 35(16): 1766–1778
35. Pilling M, Gardner P. Fundamental developments in infrared spectroscopic imaging for biomedical applications. Chem Soc Rev 2016; 45(7): 1935–1957
36. Cazaux S, Sadoun A, Biarnes-Pelicot M, Martinez M, Obeid S, Bongrand P, Limozin L, Puech PH. Synchronizing atomic force microscopy force mode and fluorescence microscopy in real time for immune cell stimulation and activation studies. Ultramicroscopy 2016; 160: 168–181
37. Knoops B, Becker S, Poncin MA, Glibert J, Derclaye S, Clippe A, Alsteens D. Specific interactions measured by AFM on living cells between peroxiredoxin-5 and TLR4: relevance for mechanisms of innate immunity. Cell Chem Biol 2018; 25(5): 550–559.e3
38. Camesano TA, Liu Y, Datta M. Measuring bacterial adhesion at environmental interfaces with single-cell and single-molecule techniques. Adv Water Resour 2007; 30(6–7): 1470–1491
39. Rana MS, Pota HR, Petersen IR. Performance of sinusoidal scanning with MPC in AFM imaging. IEEE/ASME Trans Mechatron 2015; 20(1): 73–83
40. Rana MS, Pota HR, Petersen IR. Spiral scanning with improved control for faster imaging of AFM. IEEE Trans NanoTechnol 2014; 13(3): 541–550
41. Arildsen T, Oxvig CS, Pedersen PS, Ostergaard J, Larsen T. Reconstruction algorithms in undersampled AFM imaging. IEEE J Sel Top Signal Process 2016; 10(1): 31–46
42. Heu C, Berquand A, Elie-Caille C, Nicod L. Glyphosate-induced stiffening of HaCaT keratinocytes, a Peak Force Tapping study on living cells. J Struct Biol 2012; 178(1): 1–7
43. Newton R, Müller DJ. Cells stiffen for cytokines. Cell Chem Biol 2018; 25(5): 495–496
44. Salapaka SM, Ramamoorthy A, Salapaka MV. AFM imaging? Reliable or not?: validation and verification of images in atomic force microscopy. Control Systems IEEE 2013; 33(6): 106–118
45. Smith DA, Robinson C, Kirkham J, Zhang J, Wallwork ML. Chemical force spectroscopy and imaging. Rev Anal Chem 2001; 20(1): 1–26
46. Zhang X, Wojcikiewicz EP, Moy VT. Dynamic adhesion of T lymphocytes to endothelial cells revealed by atomic force microscopy. Exp Biol Med (Maywood) 2006; 231(8): 1306–1312
47. Drew ME, Konicek AR, Jaroenapibal P, Carpick RW, Yamakoshi Y. Nanocrystalline diamond AFM tips for chemical force spectroscopy: fabrication and photochemical functionalization. J Mater Chem B Mater Biol Med 2012; 22(25): 12682–12688
48. Hyonchol K, Hideo A, Toshiya O and ATsushi I. Quantification of cell adhesion interactions by AFM: effects of LPS/PMA on the adhesion of C6 glioma cell to collagen type I. Appl Surf Sci 2002; 188(3–4): 493–498
49. Hu KH, Butte MJ. T cell activation requires force generation. J Cell Biol 2016; 213(5): 535–542
50. Nikkhah M, Strobl JS, Schmelz EM, Agah M. Evaluation of the influence of growth medium composition on cell elasticity. J Biomech 2011; 44(4): 762–766
51. Neubert E, Meyer D, Rocca F, Günay G, Kwaczala-Tessmann A, Grandke J, Senger-Sander S, Geisler C, Egner A, Schön MP, Erpenbeck L, Kruss S. Chromatin swelling drives neutrophil extracellular trap release. Nat Commun 2018; 9(1): 3767
52. Sheetz MP. Cell control by membrane-cytoskeleton adhesion. Nat Rev Mol Cell Biol 2001; 2(5): 392–396
53. Diz-Muñoz A, Fletcher DA, Weiner OD. Use the force: membrane tension as an organizer of cell shape and motility. Trends Cell Biol 2013; 23(2): 47–53
54. Maridonneau-Parini I. Control of macrophage 3D migration: a therapeutic challenge to limit tissue infiltration. Immunol Rev 2014; 262(1): 216–231

55. Bitler A, Dover R, Shai Y. Fractal properties of macrophage membrane studied by AFM. Micron 2012; 43(12): 1239–1245
56. Labernadie A, Bouissou A, Delobelle P, Balor S, Voituriez R, Proag A, Fourquaux I, Thibault C, Vieu C, Poincloux R, Charrière GM, Maridonneau-Parini I. Protrusion force microscopy reveals oscillatory force generation and mechanosensing activity of human macrophage podosomes. Nat Commun 2014; 5(1): 5343
57. Souza ST, Agra LC, Santos CEA, Barreto E, Hickmann JM, Fonseca EJS. Macrophage adhesion on fibronectin evokes an increase in the elastic property of the cell membrane and cytoskeleton: an atomic force microscopy study. Eur Biophys J 2014; 43(12): 573–579
58. Labernadie A, Thibault C, Vieu C, Maridonneau-Parini I, Charrière GM. Dynamics of podosome stiffness revealed by atomic force microscopy. Proc Natl Acad Sci USA 2010; 107(49): 21016–21021
59. Lowin B, Hahne M, Mattmann C, Tschopp J. Cytolytic T-cell cytotoxicity is mediated through perforin and Fas lytic pathways. Nature 1994; 370(6491): 650–652
60. Kägi D, Vignaux F, Ledermann B, Bürki K, Depraetere V, Nagata S, Hengartner H, Golstein P. Fas and perforin pathways as major mechanisms of T cell-mediated cytotoxicity. Science 1994; 265 (5171): 528–530
61. Kägi D, Ledermann B, Bürki K, Seiler P, Odermatt B, Olsen KJ, Podack ER, Zinkernagel RM, Hengartner H. Cytotoxicity mediated by T cells and natural killer cells is greatly impaired in perforin-deficient mice. Nature 1994; 369(6475): 31–37
62. Baran K, Dunstone M, Chia J, Ciccone A, Browne KA, Clarke CJP, Lukoyanova N, Saibil H, Whisstock JC, Voskoboinik I, Trapani JA. The molecular basis for perforin oligomerization and transmembrane pore assembly. Immunity 2009; 30(5): 684–695
63. Ding J, Wang K, Liu W, She Y, Sun Q, Shi J, Sun H, Wang DC, Shao F. Pore-forming activity and structural autoinhibition of the gasdermin family. Nature 2016; 535(7610): 111–116
64. Mukherjee S, Zheng H, Derebe MG, Callenberg KM, Partch CL, Rollins D, Propheter DC, Rizo J, Grabe M, Jiang QX, Hooper LV. Antibacterial membrane attack by a pore-forming intestinal C-type lectin. Nature 2014; 505(7481): 103–107
65. Newton R, Delguste M, Koehler M, Dumitru AC, Laskowski PR, Müller DJ, Alsteens D. Combining confocal and atomic force microscopy to quantify single-virus binding to mammalian cell surfaces. Nat Protoc 2017; 12(11): 2275–2292
66. Law RH, Lukoyanova N, Voskoboinik I, Caradoc-Davies TT, Baran K, Dunstone MA, D'Angelo ME, Orlova EV, Coulibaly F, Verschoor S, Browne KA, Ciccone A, Kuiper MJ, Bird PI, Trapani JA, Saibil HR, Whisstock JC. The structural basis for membrane binding and pore formation by lymphocyte perforin. Nature 2010; 468(7322): 447–451
67. Pasparakis M, Vandenabeele P. Necroptosis and its role in inflammation. Nature 2015; 517(7534): 311–320
68. Newton K, Wickliffe KE, Maltzman A, Dugger DL, Strasser A, Pham VC, Lill JR, Roose-Girma M, Warming S, Solon M, Ngu H, Webster JD, Dixit VM. RIPK1 inhibits ZBP1-driven necroptosis during development. Nature 2016; 540(7631): 129–133
69. Eaton P, do Amaral CP, Couto SCP, Oliveira MS, Vasconcelos AG, Borges TKS, Kückelhaus SAS, Leite JRSA, Muniz-Junqueira MI. Atomic force microscopy is a potent technique to study eosinophil activation. Front Physiol 2019; 10: 1261
70. Shen X, Gu H, Ma P, Luo Z, Li M, Hu Y, Cai K. Minocycline-incorporated multilayers on titanium substrates for simultaneous regulation of MSCs and macrophages. Mater Sci Eng C 2019; 102: 696–707
71. Pi J, Cai H, Yang F, Jin H, Liu J, Yang P, Cai J. Atomic force microscopy based investigations of anti-inflammatory effects in lipopolysaccharide-stimulated macrophages. Anal Bioanal Chem 2016; 408(1): 165–176